

Forced motion of a probe particle near the colloidal glass transition

P. HABDAS, D. SCHAAR, ANDREW C. LEVITT and ERIC R. WEEKS

Physics Department, Emory University, Atlanta, GA 30322

PACS. 82.70.Dd – colloids.

PACS. 64.70.Pf – glass transition.

PACS. 61.43.Fs – glasses.

Abstract. – We use confocal microscopy to study the motion of a magnetic bead in a dense colloidal suspension, near the colloidal glass transition volume fraction ϕ_g . For dense liquid-like samples near ϕ_g , below a threshold force the magnetic bead exhibits only localized caged motion. Above this force, the bead is pulled with a fluctuating velocity. The relationship between force and velocity becomes increasingly nonlinear as ϕ_g is approached. The threshold force and nonlinear drag force vary strongly with the volume fraction, while the velocity fluctuations do not change near the transition.

Introduction. – Near the glass transition, molecular motion is greatly slowed, yet the motion of molecules is difficult to directly observe and the character of the molecular slowing is hard to determine [1–4]. Thus, colloidal suspensions of micrometer-sized spheres are a useful model system for investigating the nature of the glass transition, as they can be directly observed using optical microscopy [5–9]. As the volume fraction of a colloidal suspension is increased, the motion of the particles becomes restricted due to the confining effect of the other particles: each particle is temporarily trapped in a “cage” formed by its neighbors [9–12]. For liquid-like samples, these cages eventually deform and allow particles to diffuse through the sample [9, 10]. Above a critical volume fraction ($\phi_g \sim 0.58$ for hard sphere colloids), the particles’ diffusion constant becomes zero and the macroscopic viscosity increases dramatically [10, 13]. A system at such state is considered a colloidal glass and ϕ_g is identified as the colloidal glass transition point. To gain insight into the nature of the colloidal glass transition, past work used optical microscopy to study the motion of individual particles as a function of volume fraction [5–9]. These experiments discovered that particle motion in equilibrated samples is both spatially heterogeneous and temporally intermittent. However, only a few studies [14, 15] have focused on nonequilibrium, driven motion.

In this Letter, we study experimentally the motion of a magnetic bead pulled through a dense colloidal suspension. Similar to previous work with magnetic probes, we are able to probe the local rheological properties of the suspension [16–18], although unlike those studies, our samples are heterogeneous on the scale of the magnetic probe. In our experiments, as the colloidal glass transition is approached the motion of the magnetic bead becomes complex. Below a threshold force, the magnetic bead exhibits only localized caged motion. When the

external force is above this threshold, the magnetic bead moves significantly faster, with a fluctuating velocity. Closer to ϕ_g , the threshold force rises, and the velocity-force relationship becomes increasingly nonlinear. Our measurements reveal dramatic changes in the drag force acting on the magnetic bead as the glass transition is approached.

Experimental. – The colloidal suspensions are made of poly-(methylmethacrylate) particles, sterically stabilized by a thin layer of poly-12-hydroxystearic acid [19]. The particles have a radius $a = 1.10 \mu\text{m}$, a polydispersity of $\sim 5\%$, and are dyed with rhodamine. The particles are slightly charged, shifting the phase transition boundaries from those of hard spheres. We observe the freezing transition at $\phi_f \approx 0.38$, the melting transition at $\phi_m \approx 0.42$, and the glass transition at $\phi_g \approx 0.58$. The glass transition is characterized by a vanishing diffusion constant for the particles' motion, measured by confocal microscopy. The colloidal particles are suspended in a mixture of cyclohexylbromide/*cis*- and *trans*- decalin which nearly matches both the density and the index of refraction of the colloidal particles. We add superparamagnetic beads with a radius of $a_{\text{MB}} = 2.25 \mu\text{m}$ (M450, coated with glycidyl ether reactive groups, Dynal), at a volume fraction $\sim 10^{-5}$, so that the magnetic beads are well separated. We do not observe attraction or repulsion between the colloidal particles and the magnetic beads, in either dilute or concentrated samples. Before beginning experiments, we mix the sample with an air bubble which breaks up any pre-existing crystalline regions, then we wait 20 minutes before taking data, to allow the air bubble to stop moving. The colloidal suspension is not observed to flow during the acquisition of the data.

With a confocal microscope [20], we rapidly acquire images (1.88 image/s) of area $80 \mu\text{m} \times 80 \mu\text{m}$, containing several hundred particles. The magnetic beads are not fluorescent and thus appear black on the background of dyed colloidal particles. To exert a force on these beads, a Neodymium magnet is mounted on a micrometer held just above the sample. The force is calibrated by determining the velocity of the magnetic beads in glycerol for a given magnet position, and inferring the drag force from Stokes' Law ($F = 6\pi\eta a_{\text{MB}}v$, where F is the drag force, η is the viscosity, and v is the observed velocity) [17]. The imperfect reproducibility of the magnet position causes a 5% uncertainty of the force. Additionally, the variability in magnetic bead composition results in an uncertainty in the magnetic force on different beads, which we measure to be less than 10%. Also, the magnetic beads are not density matched, and their effective weight is 0.1 pN. This is nearly negligible compared to the applied horizontal forces in our experiments, and so in our data below we consider only the applied forces and the measured velocities in the x direction. We observe very little vertical motion of the magnetic beads, typically less than 5% of the horizontal motion. This is less than our other measurement errors, discussed below. We study isolated magnetic beads at least $35 \mu\text{m}$ and more typically $>50 \mu\text{m}$ from the sample chamber boundary and from other magnetic beads. Our experiments are limited by crystallization as the average velocity of the magnetic bead decreases significantly in the crystallized regions. Thus, we make sure that the data are collected well before crystallization appears. Repeated measurements are reproducible before the onset of crystallization.

Results and discussion. – We study the motion of the magnetic beads for a range of forces. Within each image, we locate the center of the magnetic bead with an accuracy of at least $0.5 \mu\text{m}$ [21]. To show the behavior of the magnetic bead, we plot the average magnetic bead velocity against the applied force on a log-log plot in Fig. 1 for a range of volume fractions. The average velocity of the magnetic bead for a given F is given by $\bar{v} = \Delta x / \Delta t$ for the entire course of the measurement; the error bars in Fig. 1 are from the standard deviation of repeated measurements of \bar{v} for the same magnetic bead at the same F . For a dilute system ($\phi = 0.29$, asterisks) the data fall on a line with a slope of 1, indicating that the velocity is

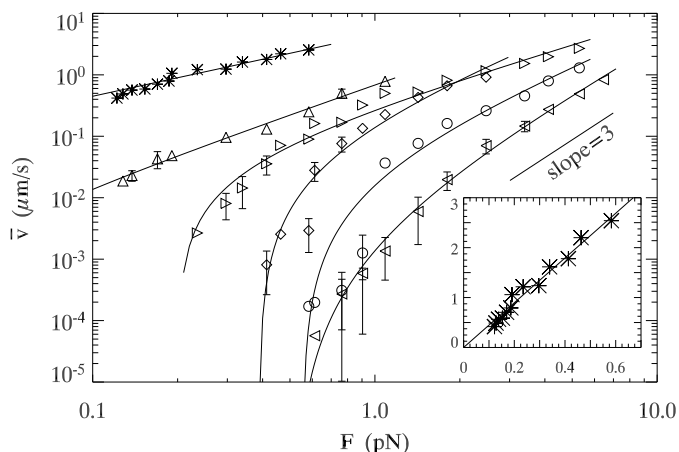


Fig. 1

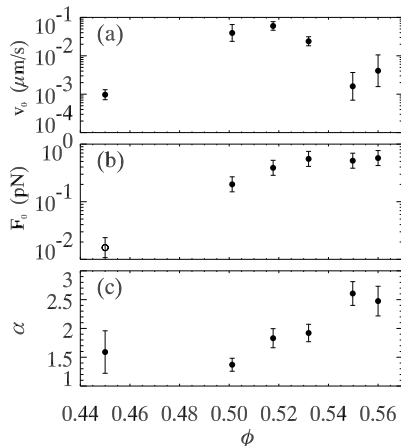


Fig. 2

Fig. 1 – Average velocity of the magnetic bead in the direction of the motion as a function of force acting on the magnetic bead for the volume fractions: 0.29 (*), 0.45 (\triangle), 0.50 (\triangleright), 0.52 (\diamond), 0.53 (\circ), 0.55 (\triangleleft). Solid lines are fits to the data obtained using Eq. (1). Each data set is taken for a single magnetic particle and thus the magnetic particle variability may shift curves relative to each other but does not influence the shape of a curve for a given volume fraction. The velocity error due to the uncertainty in the bead position is 5%, smaller than the symbol size. The slope=3 line is added for comparison. Inset: Data for $\phi = 0.29$ on a linear/linear plot.

Fig. 2 – Fitting parameters as a function of volume fraction: (a) V_0 , (b) threshold force F_0 , and (c) power exponent α . The error bars are due to the uncertainties in measuring the forces and velocities that the model is fit to. The solid symbols for F_0 correspond to data sets for which stalled behavior was directly observed below F_0 (all data sets $\phi \geq 0.50$).

linearly proportional to the applied force and Stokes’ law applies (Fig. 1 inset). Due to the nonzero volume fraction, the effective viscosity is modified from that of the solvent ($\eta_0 = 2.25$ mPa·s) to the larger value of $\eta = 6 \pm 1$ mPa·s, in reasonable agreement with past macroscopic measurements [13].

At higher volume fractions the velocity-force relationship becomes more complex (Fig. 1). For data at large forces, the average velocity seems to grow as a power law with force, $\bar{v} \sim F^\alpha$, with exponent α between 1.5 and 3. From left to right the curves increase in volume fraction, and the slope at the highest forces for each curve increases nearly monotonically, reflecting the approach of the glass transition. For all samples $\phi \geq 0.50$, we took data at extremely low forces, and found that the magnetic bead did not move more than our resolution limit within four hours; instead, it exhibits random caged motion. This observation time is limited by the onset of crystallization of the sample; in other words, the velocity is smaller than $4 \cdot 10^{-5}$ $\mu\text{m/s}$. Since the colloidal particles move due to Brownian motion one would expect rearrangements to “allow” for the magnetic bead to move, even if this motion would be primarily random with a small bias from the external force. However, within our observation time scale we cannot see this behavior, and conclude that the velocity of such a random walk is quite small. For $\phi = 0.29$ and 0.45, for all forces checked, motion of the magnetic bead was observed. (Forces below 0.1 pN are unobtainable, as this is the effective weight of the magnetic bead.)

To determine how the velocity/force relationship changes as the volume fraction is in-

creased, we fit the data to the following equation:

$$\begin{aligned}\bar{v} &= v_0 \cdot \left(\frac{F}{F_0} - 1\right)^\alpha, & F > F_0 \\ &= 0, & F \leq F_0\end{aligned}\quad (1)$$

where F_0 is a threshold force and α is the exponent characterizing the growth of the velocity at large forces. v_0 is the velocity the magnetic bead would have if the applied force F was equal to $2F_0$. This functional form was also used to fit data from a two-dimensional simulation similar to our experiments [22]. The solid lines in Fig. 1 are the results of fitting the data with Eq. (1), with the exception of the $\phi = 0.29$ data (asterisks) where Stokes' Law applies. While the model seems a good fit to our data, our data are not strong enough to verify the model. However, the model provides a useful way to quantify the main features of the data.

As the colloidal glass transition is approached the system becomes more viscous, and this is reflected in the changing fit parameters from Eq. (1) shown in Fig. 2. For low volume fractions, the three parameters v_0 , F_0 , and α are all small, and Stokes' Law may be the simplest explanation for the force/velocity data. The fit parameters change as the volume fraction $\phi \rightarrow \phi_g$. v_0 initially grows with increasing ϕ and then drops [Fig. 2(a)]. The initial increase presumably reflects the change from the $v_0 \rightarrow 0$ limit at low volume fractions. The decrease as the glass transition is approached may be due to the sharply increasing effective viscosity acting on the magnetic bead. v_0 is also sensitive to variations in the other fitting parameters, as for large F , $v \approx (v_0 F_0^{-\alpha}) F^\alpha$.

The threshold force F_0 grows as ϕ increases, reaching a plateau value for large ϕ . We expect that at ϕ_g the threshold force will be finite, both from our data, and also as it seems more likely that F_0 diverges at $\phi_{\text{RCP}} \approx 0.64$, the random close-packing volume fraction [13]. The value of the threshold force near ϕ_g , $F_0 \sim 1$ pN, is similar to that predicted by the work of Schweizer and Saltzman *et al.* [11,12]. They determined an effective free energy characterizing caged particle motion, and the derivative of this energy can be used to find an effective force to break out of a cage, resulting in a value of $\approx 50k_B T/a \approx 0.2$ pN for $\phi = 0.6$ [11,12]. This prediction considers the caged particle to be the same size as the surrounding particles, and for our larger magnetic beads the stall force would likely be larger, closer to our experimental values. Thus, our measured threshold forces F_0 may be related to the strength of colloidal cages; previously only the sizes of these cages have been measured [9,10].

The exponent α changes dramatically as the glass transition is approached, as seen in Fig. 2(c), where it rises to almost 3 near ϕ_g . Our results are in contrast to Ref. [22]; while the model fits their data as well, they found $\alpha = 1.5$ for glassy systems. The difference may be due to the much different particle interactions: they studied unscreened point charges in a 2D system, qualitatively different from our colloidal particles. In our experiments, it is unclear if α diverges at ϕ_g or continues to grow as ϕ_{RCP} is approached. Experiments at $\phi > \phi_g$ are difficult to interpret due to the aging of the sample [23]: for a given force the magnetic bead response depends on the age of the sample.

The motion of the magnetic bead is not smooth, as is seen by a typical plot of its position as a function of time [Fig. 3(a,b)]. While the largest "jumps" seen in Fig. 3(a) are roughly the diameter of the surrounding colloidal particles ($2a \sim 2 \mu\text{m}$), at other times the magnetic bead takes much smaller steps. When the magnetic bead moves faster the fluctuations become less significant and the motion of the magnetic bead is smoother, shown in Fig. 3(b).

We arbitrarily choose $\Delta t = a_{\text{MB}}/\bar{v}$ as a time scale and define the instantaneous velocity as $\vec{v}(t) = [\vec{r}(t + \Delta t) - \vec{r}(t)]/\Delta t$. This time scale is indicated with the scale bars shown in Fig. 3(a,b), and the results that follow are not sensitive to this choice (and in particular do not change using a rather than a_{MB}). The instantaneous velocity is shown in Fig. 3(c). The

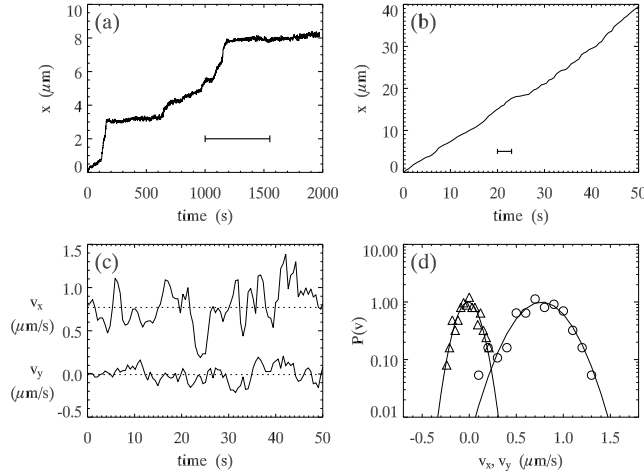


Fig. 3 – (a) The position of the magnetic bead in the direction of the motion as a function of time, $F = 0.58$ pN, $\phi = 0.52$, $v = 0.0041$ $\mu\text{m/s}$. The scale bar corresponds to $a_{\text{MB}}/v = 550\text{s}$. (b) The position of the magnetic bead in the direction of the motion as a function of time, $F = 6.46$ pN, $\phi = 0.55$, $v = 0.80$ $\mu\text{m/s}$. The scale bar corresponds to $a_{\text{MB}}/v = 3$ s. (c) The instantaneous velocity in the direction of motion v_x and perpendicular to the motion v_y as a function of time. The velocities are calculated from the displacement data using $\Delta t = 3$ s. The dashed lines denote the average velocities $\bar{v}_x = 0.80$ $\mu\text{m/s}$ and $\bar{v}_y = 0.01$ $\mu\text{m/s}$. The data are the same as (b). (d) The probability distribution of the instantaneous velocities v_x (o) and v_y (Δ). The solid lines denote a Gaussian fit with $\sigma_{v_x} = 0.24$ $\mu\text{m/s}$ and $\sigma_{v_y} = 0.10$ $\mu\text{m/s}$. The data are the same as (b).

magnetic bead velocity has much larger fluctuations along the direction of motion [v_x , top trace in Fig. 3(c)], while fluctuations in the transverse direction are smaller. The distributions of v_x and v_y , shown on Fig. 3(d), are Gaussian (solid fit lines). The fluctuations in x and y appear to be only weakly correlated. The velocity fluctuations reflect the fact that the magnetic bead is of similar size to the colloidal particles: its motion is sensitive to colloidal particle configurations. Furthermore, dense colloidal suspensions are spatially heterogeneous systems [5,6] and some regions may be “glassier” and thus harder to move through.

As the glass transition is approached, the spatial heterogeneity increases [5,6], and one might expect that the velocity fluctuations would become more significant. However, this is not the case, as is seen in Fig. 4 which shows the standard deviation of the instantaneous velocity σ_{v_x} plotted against the average velocity \bar{v} . Different symbols indicate different volume fractions, showing that it is not the volume fraction which determines the standard deviation but the average velocity: the fluctuations are larger when the average velocity is larger. Denser suspensions have slower velocities for the same force (as seen in Fig. 1) but also correspondingly smaller velocity fluctuations. In Fig. 4, the data are more scattered at low velocities and for any given sample the data scatter on both sides of the fit line. For different choices of Δt , we find that $\sigma_{v_x} \sim \bar{v}^\beta$ with the exponent $\beta = 0.8 \pm 0.1$. The smaller the Δt the wider distribution of σ_{v_x} . However, the general dependence of σ_{v_x} on \bar{v} does not depend on Δt . We find that $\sigma_{v_y} \approx 0.4\sigma_{v_x}$ and thus a similar trend holds for the transverse fluctuations.

The changing character of the motion as the glass transition is approached can be understood by calculating the modified Peclet number. This is the ratio of two time scales, τ_B characterizing the unforced motion of the colloidal particles, and τ_M characterizing the motion of the magnetic bead. The Brownian time $\tau_B = a^2/2D_\infty$ is the time it takes for colloidal

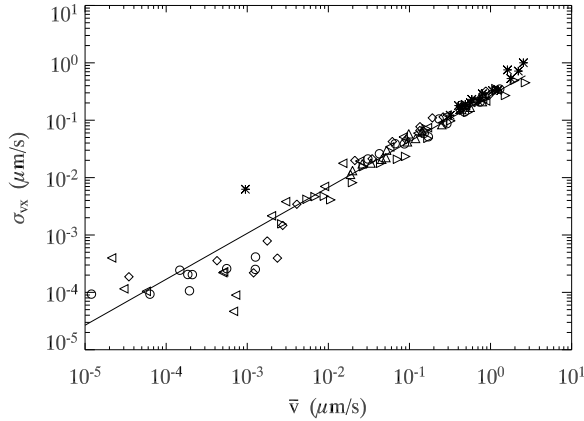


Fig. 4 – The standard deviation of the instantaneous distribution of v_x , (σ_{v_x}) as a function of \bar{v} . The solid line is a fit to the data and has a slope of 0.80. The symbols represent the different volume fractions which are the same as Fig. 1.

particles to diffuse a distance equal to their radius a and is based on their asymptotic diffusion constant D_∞ . D_∞ becomes small near the glass transition and becomes zero for a colloidal glass. The magnetic bead time scale $\tau_M = a/\bar{v}$ is the time scale for the magnetic bead to move the distance a and is based on the magnetic bead's average velocity \bar{v} . The modified Peclet number is $Pe^* = \tau_B/\tau_M$ and is larger than 1 for all symbols shown in Fig. 1 [24]. For the largest forces, $Pe^* \approx 10000$. Thus, the forced motion of the magnetic bead is much more significant than the Brownian motion of the surrounding colloidal particles: the magnetic bead pushes these particles out of the way, plastically rearranging the sample. This results in a lowering of the effective viscosity acting on the magnetic bead at higher velocities. On the macroscopic scale, this may correspond to traditional rheological measurements at high strains. Past work found for similar colloidal samples that the viscoelastic moduli decreased as the maximum strain increased [25].

For extremely low forces, $Pe < 1$ and the velocity should be linearly related to the force. However, the velocities predicted by linear response theory are well below what we observe (and for low forces, below what we can measure). This is not surprising, as the lowest forces we can apply are fairly large; a nondimensional way to characterize this is the ratio $a_{MB}F/k_B T$ which is ~ 50 for $F=0.1$ pN.

Since $Pe^* > 1$ in our experiments, the Brownian motion should be unimportant, similar to a granular system. Moreover, conjectures of the existence of a “jamming transition” speculate that the colloidal glass transition is similar to jamming in granular media [26], and so it is interesting to compare our results with studies performed in a granular media. Albert *et al.* [27] immersed a cylinder in granular particles and measured the force exerted on the cylinder when it moved with constant speed relative to the particles. They found that the drag force on the cylinder is independent of the velocity, quite different from our behavior (Fig. 1). In our experiments, the solvent viscosity may be important, causing the velocity dependent drag force.

In conclusion, we find that near the glass transition the motion of a microsphere through a colloidal suspension changes dramatically. A threshold force appears, below which the motion of the sphere is localized, and this threshold force increases as the glass transition is approached. The existence of the threshold force hints that the system may locally “jam”

even when the colloidal suspension is globally still a liquid. Above the threshold force the velocity is related to the force by a power law and the sphere moves with a fluctuating velocity, locally deforming the sample. At high forces, the velocity is related to the force by a power law. This can be inverted to obtain an effective drag force on the sphere, growing weakly with velocity, $F \sim v^{1/\alpha}$ with α growing from 1 far from the glass transition to nearly 3 close to the transition. These results indicate that the approach of the colloidal glass transition is signaled by a growing nonlinearity of the drag force. This may be a new way to characterize the glass transition and should serve as a useful test for some glass transition theories [11, 12, 28, 29].

We thank R. E. Courtland, M. B. Hastings, S. A. Koehler, D. Nelson, K. S. Schweizer, T. Squires, T. A. Witten, and S. Wu for helpful discussions. We thank A. Schofield for providing our colloidal samples. This work was supported by NASA (NAG3-2284).

REFERENCES

- [1] EDIGER M. D., ANGELL C. A. and NAGEL S. R., *J. Phys. Chem.*, **100** (1996) 13200.
- [2] ANGEL C. A., *Science*, **267** (1995) 1924.
- [3] STILLINGER F. H., *Science*, **267** (1995) 1935.
- [4] ANGELL C. A., *J. Phys. Cond. Mat.*, **12** (2000) 6463.
- [5] KEGEL W. K. and VAN BLAADEREN A., *Science*, **287** (2000) 290.
- [6] WEEKS E. R., CROCKER J. C., LEVITT A. C., SCHOFIELD A. and WEITZ D.A., *Science*, **287** (2000) 627.
- [7] MARCUS A. H., SCHOFIELD J. and RICE S. A., *Phys. Rev. E*, **60** (1999) 5725.
- [8] KASPER A., BARTSCH E. and SILLESCU H., *Langmuir*, **14** (1998) 5004.
- [9] WEEKS E. R. and D. A. WEITZ, *Phys. Rev. Lett.*, **89** (2002) 095704.
- [10] VAN MEGEN W., MORTENSEN T. C., WILLIAMS S. R., MULLER J., *Phys. Rev. E*, **58** (1998) 6073.
- [11] SCHWEIZER K. S., SALTZMAN E. J., *J. Chem. Phys.*, **119** (2003) 1181.
- [12] Schweizer K. S., private communication.
- [13] CHENG Z., ZHU J., CHAIKIN P. M., PHAN S.-E., and RUSSEL W. B., *Phys. Rev. E*, **65** (2002) 041405-1.
- [14] STRATING P., *Phys. Rev. E*, **59** (1999) 2175.
- [15] MARANZANO B. J. and WAGNER N. J., *J. Chem. Phys.*, **114** (2001) 10514.
- [16] AMBLARD F., YURKE B., PARGELLIS A. and LEIBLER S., *Rev. Sci. Instr.*, **67** (1996) 818.
- [17] KELLER M., SCHILLING J. and SACKMANN E., *Rev. Sci. Instr.*, **72** (2001) 3626.
- [18] WILHELM C., BROWAEYS J., PONTON A. and BACRI J.-C., *Phys. Rev. E*, **67** (2003) 011504-1.
- [19] ANTL L., GOODWIN J. W., HILL R. D., OTTEWILL R. H., OWENS S. M., PAPWORTH S. and WATERS J. A., *Colloids Surf*, **17** (1986) 67.
- [20] DINSMORE A. D., WEEKS E. R., PRASAD V., LEVITT A. C., and WEITZ D. A., *App. Opt.*, **40** (2001) 4152.
- [21] CROCKER J. C. and GRIER D. G., *J. Colloid Interface Sci.*, **179** (1996) 298.
- [22] HASTINGS M. B., OLSON REICHHARDT C. J. and REICHHARDT C., *Phys. Rev. Lett.*, **90** (2003) 098302-1.
- [23] COURTLAND R. E. and WEEKS E. R., *J. Phys. Cond. Mat.*, **15** (2003) S359.
- [24] We term this the “modified” Peclet number as we are using D_∞ rather than D_0 , the diffusion constant characterizing particle motion in dilute samples.
- [25] MASON T. G. and WEITZ D. A., *Phys. Rev. Lett.*, **75** (1995) 2770.
- [26] LIU A. J. and NAGEL S. R., *Nature*, **396** (1998) 21.
- [27] ALBERT R., PFEIFER M. A., BARABASI A.-L. and SCHIFFER P., *Phys. Rev. Lett.*, **82** (1999) 205.
- [28] FALK M. L. and LANGER J. S., *Phys. Rev. E*, **57** (1998) 7192.
- [29] BERTHIER L. and BARRAT J.-L., *Phys. Rev. Lett.*, **89** (2002) 095702-1.